Smart Noise Jamming Suppression Technique Based on Blind Source Separation

Wen Yu and Wei Chen
School of Electronic Information Engineering, Beihang University, Beijing, China
Email: wenyuyuwen@126.com, chenwei@buaa.edu.cn

***Abstract*—Smart noise jamming is one of radar active jamming modes, which has the characteristics of both suppression and deception. When it is used as self-defense jamming, radar target detection will be threatened greatly. Blind source separation (BSS) is proposed to solve the problem of multiplicative modulation smart noise jamming and target echo mixture to suppress the interference. Firstly, the receiving channel is expanded by the auxiliary antenna whose polarized mode is orthogonal to the main antenna of radar, and the problem of single channel is transformed into multi-channel. Secondly, weights-adjusted second-order blind identification (WASOBI) is utilized to separate the jamming and target echo. To decrease the influence of channel noise on BSS, wavelet de-noising is used on the observed signals. The simulation shows that when SNR is greater than 15dB, the similarity coefficient of target echo obtained by BSS can reach more than 0.85 after de-noising process.**

***Index Terms*—smart noise jamming, polarized channel expanding, BSS, self-defense jamming, wavelet de-noising**

I. Introduction

In modern electronic warfare, with the development of digital radio frequency memory (DRFM) technology, complex operations can be conducted on radar signals which are intercepted by jammer, including replication, time domain modulation and retransmission. Smart noise jamming is a new radar active jamming mode which is proposed on this background. It has many different signal forms. In general, smart noise jamming is usually obtained by multiplicative or convolutional modulation of the intercepted radar transmitted signal. This jamming is in good coherence with target echo and can obtain the processing gain of radar. It has the characteristics of both suppressive and deceptive radar jamming. Interference suppression measures like sidelobe cancellation and sidelobe blanking can be effectively impaired by smart noise jamming [1]. To combat smart noise jamming, adaptive sidelobe cancellation technique is proved to suppress convolutional smart noise jamming efficiently in [2]. Smeared spectrum (SMSP) technique and atomic decomposition is utilized by [3] to inhibit convolutional smart noise jamming. Overall, research on the multiplicative smart noise is less. The circumstance where the interference enters the main lobe and signal processing is used to accomplish anti-jamming is less discussed.

When smart noise jamming is used in self-defense jamming, the target echo and the jamming signal come from the same direction and enter the radar receiving antenna from the main lobe. Both of them cannot be distinguished in time domain, frequency domain and spatial domain. BSS is a signal processing method for separating aliasing signals. It can be used to separate the target echo from the jamming signal to achieve the purpose of anti-jamming. In the present research of radar anti-jamming, when target echo and jamming signal are received by single channel (e.g self-defense jamming), channel expansion is mainly used to simplify the problem to positive definite BSS. Ref. [4] and [5] use two methods of virtual channel expansion to realize separation. However, these two channel extensions can only solve the single delay deception interference. The multi-channel expansion is carried out by sampling on multiple pulse repetition periods (PRI), and then dense false target jamming and target echo are separated by joint approximate diagonalization of eigenmatrices (JADE) in [6]. It is required that the target should not cross the range gate in multiple PRIs. A new channel expansion technique is designed in [7]. It uses the difference of polarization characteristics between auxiliary antenna and main antenna. By using channel entity expansion to construct two mixed signals, shift-frequency jamming and target echo are separated successfully.

In this paper, we aim at the scene where smart noise jamming is used as self-defense jamming. The second mixed signal is constructed through using the auxiliary antenna whose polarized mode is orthogonal to the main antenna of radar [7]. Then, a BSS algorithm called WASOBI is chosen to separate the smart noise jamming from the target echo. The smart noise jamming in this work refers to the jamming mode in [8], which uses the local narrowband noise in jammer to multiply with the intercepted radar transmitted signal. The target distance information can be obtained by pulse compression for the separated target echo. Finally, wavelet de-noising is utilized to improve the performance of BSS when signal-to-noise ratio (SNR) is low.

II. Description of Problem

A. Modeling of Radar Receiving Signals

Assuming that radar transmits LFM signals:

Manuscript received December 26, 2018; revised February 16, 2019.

doi: 10.18178/ijsps.7.1.14-19

$$s(t) = rect(\frac{t}{T})e^{j\phi_T(t)} \tag{1}$$

where T is pulse width, $\phi_T(t) = 2\pi f_0 t + \pi K t^2$, f_0 and K are central frequency and chirp rate of the signal, respectively. The target echo can be expressed as:

$$S_r(t) = ae^{j\varphi_T} rect(\frac{t-\tau_T}{T})e^{j[\phi_T(t-\tau_T)+2\pi f_d^T(t-\tau_T)]}$$
$$= ae^{j\varphi_T} S'(t) \tag{2}$$

where a is the amplitude of target echo. φ_T is the initial phase of target echo and has uniform distribution in $(-\pi,\pi)$. $\tau_T = 2R_j / C$, R_j is the distance between radar and target, which carries jammer. C and f_d^T are velocity of light and doppler shift of target, respectively.

The model of smart noise jamming is:

$$J(t) = be^{j\varphi_J}\left\{rect(\frac{t}{T})e^{j[\phi_T(t)+2\pi f_d^T t]} \times n(t)\right\} \otimes \delta(t-\tau_T-\tau_J)$$
$$= be^{j\varphi_J} J'(t) \tag{3}$$

where b is the amplitude of jamming signal. φ_J is the initial phase of smart noise jamming and has uniform distribution in $(-\pi,\pi)$. τ_J is jammer's retransmission delay, $n(t)$ is the narrow band noise produced by the jammer.

Auxiliary antennas are often set in sidelobe cancellation technique. When the polarization mode of the main and auxiliary antenna is orthogonal, self-defense jamming can be suppressed [9]. In this paper, the second channel mixed signal is constructed by the auxiliary antenna which is orthogonal to the polarization mode of the radar main antenna. Therefore, the single channel BSS problem caused by the self-defense jamming is transformed into a positive definite case, which simplifies the problem.

At the radar receiving antenna port, the target echo and jamming signals can be expressed as [7]:

$$e_r(t) = \boldsymbol{S_p h_m}\sqrt{\frac{P_t g_m^2 \lambda^2 \sigma}{(4\pi)^3 R_j^4}} S_r(t)$$
$$= \boldsymbol{S_p h_m}\sqrt{\frac{P_t g_m^2 \lambda^2 \sigma}{(4\pi)^3 R_j^4}} ae^{j\varphi_T} S'(t) \tag{4}$$

$$e_J(t) = \boldsymbol{h_j}\sqrt{\frac{P_j g_m \lambda^2}{(4\pi R_j)^2}} J(t)$$
$$= \boldsymbol{h_j}\sqrt{\frac{P_j g_m \lambda^2}{(4\pi R_j)^2}} be^{j\varphi_T} J'(t) \tag{5}$$

where $\boldsymbol{S_p} = \begin{bmatrix} S_{HH} & S_{VH} \\ S_{HV} & S_{VV} \end{bmatrix}$ is the polarization scattering matrix of target. $\boldsymbol{h_m} = [h_{mH}, h_{mV}]^T$ is the polarization vector of radar main antenna, $\|\boldsymbol{h_m}\| = 1$. $\boldsymbol{h_j} = [h_{jH}, h_{jV}]^T$ is the polarization vector of jammer's transmitting antenna, $\|\boldsymbol{h_j}\| = 1$. P_t is the power of radar transmitted signal. g_m is the radar main antenna gain at current orientation. λ is radar wavelength and P_j is the transmission power of jammer. σ is the RCS of target.

Therefore, the voltage signal entering the radar main antenna and auxiliary antenna can be respectively obtained as:

$$v_m(t) = \boldsymbol{h_m^T}[e_r(t) + e_j(t)] \tag{6}$$

$$= \boldsymbol{h_m^T}[\boldsymbol{S_p h_m}\sqrt{\frac{P_t g_m^2 \lambda^2 \sigma}{(4\pi)^3 R_j^4}} ae^{j\varphi_T} S'(t) + \boldsymbol{h_j}\sqrt{\frac{P_j g_m \lambda^2}{(4\pi R_j)^2}} be^{j\varphi_T} J'(t)]$$

$$v_a(t) = \boldsymbol{h_a^T}[e_r(t) + e_j(t)] \tag{7}$$

$$= \boldsymbol{h_a^T}[\boldsymbol{S_p h_m}\sqrt{\frac{P_t g_m g_a \lambda^2 \sigma}{(4\pi)^3 R_j^4}} ae^{j\varphi_T} S'(t) + \boldsymbol{h_j}\sqrt{\frac{P_j g_a \lambda^2}{(4\pi R_j)^2}} be^{j\varphi_J} J'(t)]$$

where $\boldsymbol{h_a} = [h_{aH}, h_{aV}]^T$ is the polarization vector of the orthogonal polarization auxiliary antenna, $\|\boldsymbol{h_a}\| = 1$. g_a is the radar auxiliary antenna gain at current orientation.

From (6) and (7), it can be seen that:

$$\begin{bmatrix} v_m(t) \\ v_a(t) \end{bmatrix} = \begin{bmatrix} \boldsymbol{h_m^T S_p h_m}\sqrt{\frac{P_t g_m^2 \lambda^2 \sigma}{(4\pi)^3 R_j^4}} & \boldsymbol{h_m^T h_j}\sqrt{\frac{P_j g_m \lambda^2}{(4\pi R_j)^2}} \\ \boldsymbol{h_a^T S_p h_m}\sqrt{\frac{P_t g_m g_a \lambda^2 \sigma}{(4\pi)^3 R_j^4}} & \boldsymbol{h_a^T h_j}\sqrt{\frac{P_j g_a \lambda^2}{(4\pi R_j)^2}} \end{bmatrix} \times$$

$$\begin{bmatrix} ae^{j\varphi_T} & 0 \\ 0 & be^{j\varphi_J} \end{bmatrix}\begin{bmatrix} S'(t) \\ J'(t) \end{bmatrix} = \boldsymbol{A}\begin{bmatrix} S'(t) \\ J'(t) \end{bmatrix} \tag{8}$$

(8) can be simplified to matrix as:

$$\boldsymbol{X}(t) = \boldsymbol{AS}(t) \tag{9}$$

So far, the positive definite linear mixed model based on polarization channel expansion is completed. $\boldsymbol{A}$ is a 2×2 mixing matrix. $S'(t)$ and $J'(t)$ are original signals, $v_m(t)$ and $v_a(t)$ are observed signals received by the main and auxiliary antennas, respectively.

B. Elaboration of Signal Separable Condition

BSS algorithms based on independent component analysis (ICA) mainly have several separable conditions as below [10]. Firstly, the source signals must be mutually statistical independent. Secondly, the mixing matrix must be full-rank. Thirdly, at most one signal in the source signals is Gauss distribution.

Since the target echo and jamming signal are processed into the radar receiving antenna by the target reflection and jammer respectively, they can be considered independent of each other. In practice, most battle radars adopt horizontal or vertical polarization. In order to avoid the extreme loss caused by polarization mismatch, the jammer antenna is usually designed as circular polarization. Also, the polarization scattering matrix of the target changes with the attitude of the target. Therefore, at the receiving port of the main and auxiliary antenna, the polarization state of the target echo signal and the jamming signal is different. Since the polarization mode of main and auxiliary antenna is orthogonal, the mixing matrix is column full-rank [7]. Last but not least, both target echo and smart noise jamming are intra-pulse modulated signals, not Gaussian signals, and their power spectral density functions are different. Combined with the above points, target echo and smart noise jamming can be separated by BSS algorithms.

III. WASOBI Algorithm

WASOBI is an improvement of SOBI and is proposed by Petr Tichavsk [11], [12]. It mainly utilizes the second-order statistical properties of signals and transforms the least square problem of SOBI into the weighted least square problem by adding the weight matrix $\boldsymbol{V}$. With this improvement, every non-zero delay covariance matrix can be diagonalized to the maximum extent. WASOBI converges fast and is suitable for real-time signal processing. WASOBI flow chart is shown in Fig. 1. WASOBI consists of two main algorithms: uniformly weighted exhaustive diagonalization with Gauss iterations (UWEDGE) and weighted exhaustive diagonalization with Gauss iterations (WEDGE).

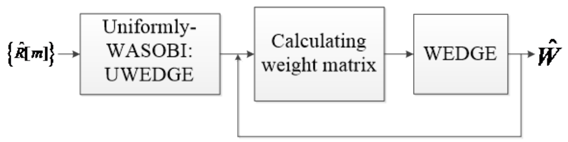

Figure 1. WASOBI algorithm flow chart.

A. UWEDGE

The delay covariance matrix of the source signal is defined as $\boldsymbol{R_S}[m] = diag\left\{r_s^{(1)}[m], r_s^{(2)}[m], \ldots, r_s^{(N)}[m]\right\}$, where m denotes the delay, m=0,1,2,…,M-1. If source signals can be simulated by Gaussian autoregressive (AR) process, then m-1 is the maximum order of Gaussian AR process. Since it is assumed that the source signals are statistically independent, the standard diagonal matrix $\boldsymbol{R_S}[m]$ is diagonal. For mixed signals $\boldsymbol{X}(t) = [x_1(t), x_2(t), \ldots, x_N(t)]^T$, the delay covariance matrix is $\hat{\boldsymbol{R}}_{\boldsymbol{X}}[m] = \frac{1}{K}\sum_{t=1}^{K} x[t]x^T[t+m]$, where m=0,1,2…,M-1. The relationship between the source signal delay matrix and the mixed signal delay matrix satisfies:

$$\hat{\boldsymbol{R}}_{\boldsymbol{X}}[m] \approx \boldsymbol{A}\hat{\boldsymbol{R}}_{\boldsymbol{S}}[m]\boldsymbol{A}^T \tag{10}$$

$$\hat{\boldsymbol{W}}\hat{\boldsymbol{R}}_{\boldsymbol{X}}[m]\hat{\boldsymbol{W}}^T \approx \hat{\boldsymbol{R}}_{\boldsymbol{S}}[m] \tag{11}$$

where $\hat{\boldsymbol{W}}$ is the estimated demixing matrix, $\boldsymbol{A}$ is the mixing matrix. When the joint diagonalization is conducted precisely, (10) and (11) are equivalent, and the estimated demixing matrix satisfies $\hat{\boldsymbol{W}} = \boldsymbol{A}^{-1}$. Because joint diagonalization is approximate, (10) and (11) are still different. Combine the two formulas together and use the least squares criterion to define them as follows:

$$\tilde{C}_{LS}(\boldsymbol{W}, \boldsymbol{A}) = \sum_{m=0}^{M-1} \left\| \boldsymbol{W}\hat{\boldsymbol{R}}_{\boldsymbol{X}}[m]\boldsymbol{W}^T - \boldsymbol{A}\boldsymbol{D}_{m,W}\boldsymbol{A}^T \right\|_F^2 \tag{12}$$

where $\boldsymbol{D}_{m,W} = ddiag(\boldsymbol{W}\hat{\boldsymbol{R}}_{\boldsymbol{X}}[m]\boldsymbol{W}^T)$. *ddiag* uses diagonal elements of the matrix in parentheses to form a new diagonal matrix. $\|\boldsymbol{A}\|_F = \sqrt{\sum_{i=1}^{m}\sum_{j=1}^{n}|a_{ij}|^2}$. a_{ij} is an element in $\boldsymbol{A}$, m and n are row and column number of a matrix. In order to make $\tilde{C}_{LS}(\boldsymbol{W}, \boldsymbol{A})$ reach the minimum, we define:

$$\Theta(\boldsymbol{W}) = \arg\min_A \tilde{C}_{LS}(\boldsymbol{W}, \boldsymbol{A})$$

$$= \arg\min_A \sum_{m=0}^{M-1} \left\| \boldsymbol{W}\hat{\boldsymbol{R}}_{\boldsymbol{X}}[m]\boldsymbol{W}^T - \boldsymbol{A}\boldsymbol{D}_{m,W}\boldsymbol{A}^T \right\|_F^2 \tag{13}$$

$\arg\min_a(\bullet)$ represents value a when the function in parentheses reach the minimum. (13) indicates that given a demixing matrix $\boldsymbol{W}$, the $\boldsymbol{A}$ value which minimizes (12) can be denoted as $\Theta(\boldsymbol{W})$. When $\Theta(\boldsymbol{W}) = \boldsymbol{I}$, $\tilde{C}_{LS}(\boldsymbol{W}, \boldsymbol{A})$ reaches the minimum, which means that $\left\{\boldsymbol{W}\hat{\boldsymbol{R}}_{\boldsymbol{X}}[m]\boldsymbol{W}^T\right\}$ can no longer be diagonalized. Simultaneously, $\boldsymbol{R_S}[m]$ is diagonalized to the maximal degree. The independent component separation is achieved. The target function of UWEDGE algorithm is $\Theta(\boldsymbol{W}) = \boldsymbol{I}$.

B. WEDGE

To improve the separation performance, the weight matrix $\boldsymbol{V}$ is added to the joint diagonalization criterion, and UWEDGE algorithm is improved to the weighted least squares criterion. (12) is rewritten as follows:

$$\tilde{C}_{VLS}(\boldsymbol{W}, \boldsymbol{A}) = [\hat{\boldsymbol{r}}_{\boldsymbol{S}}(\boldsymbol{W}) - \boldsymbol{f}(\boldsymbol{A})]^T \boldsymbol{V}[\hat{\boldsymbol{r}}_{\boldsymbol{S}}(\boldsymbol{W}) - \boldsymbol{f}(\boldsymbol{A})] \tag{14}$$

where $\hat{\boldsymbol{r}}_{\boldsymbol{S}}(\boldsymbol{W})$ and $\boldsymbol{f}(\boldsymbol{A})$ are constructed as (15)-(19):

$$\hat{\boldsymbol{r}}_{\boldsymbol{S}}(\boldsymbol{W}) = [\hat{r}_{21}^T, \hat{r}_{31}^T, \ldots, \hat{r}_{N1}^T, \hat{r}_{32}^T, \ldots, \hat{r}_{N2}^T, \ldots, \hat{r}_{N,N-1}^T]^T \tag{15}$$

$$\boldsymbol{f}(\boldsymbol{A}) = [f_{21}^T, f_{31}^T, \ldots, f_{N1}^T, f_{32}^T, \ldots, f_{N2}^T, \ldots, f_{N,N-1}^T]^T \tag{16}$$

$$\hat{\boldsymbol{r}}_{kl}(\boldsymbol{W}) = [(\boldsymbol{W}\hat{\boldsymbol{R}}_{\boldsymbol{X}}[0]\boldsymbol{W}^T)_{kl}, \ldots, (\boldsymbol{W}\hat{\boldsymbol{R}}_{\boldsymbol{X}}[M-1]\boldsymbol{W}^T)_{kl}]^T \tag{17}$$

$$\boldsymbol{f}_{kl}(\boldsymbol{A}) = [(\boldsymbol{A}\boldsymbol{D}_{0,W}\boldsymbol{A}^T)_{kl}, \ldots, (\boldsymbol{A}\boldsymbol{D}_{M-1,W}\boldsymbol{A}^T)_{kl}]^T \tag{18}$$

$$\boldsymbol{D}_{m,W} = ddiag(\boldsymbol{W}\hat{\boldsymbol{R}}_{\boldsymbol{X}}[m]\boldsymbol{W}^T) \tag{19}$$

where k, l=1,2,…,N and $k>l$. Similarly, (13) can be changed into:

$$\Theta_V(\boldsymbol{W}) = \arg\min_{\boldsymbol{A}} \tilde{C}_{VLS}(\boldsymbol{W}, \boldsymbol{A}) \tag{20}$$

The target function of WEDGE algorithm is rewritten as $\Theta_V(\boldsymbol{W}) = \boldsymbol{I}$.

C. Specific Process of WASOBI

To reduce the WEDGE algorithm complexity, the Gauss iteration method is adopted [12]. Steps of WEDGE are shown below:

Step1: Calculate $\hat{\boldsymbol{R}}_X[m], m = 0,1,2,...,M-1$. The weight matrix $\boldsymbol{V}$ can be any nonzero matrix. Also, the optimal weight matrix $\boldsymbol{V}$ can be calculated according to the preliminary separated independent component obtained by UWEDGE. The optimal weight matrix is defined as $\boldsymbol{V} = \boldsymbol{\Phi}^{-1}$. $\boldsymbol{\Phi}$ is the estimated covariance matrix based on the preliminary separated source signal. There are $N(N-1)/2$ weight matrices, in the form of $\boldsymbol{V}_{kl} \in \boldsymbol{R}^{M\times M}$, k,l=1,2,…,N, $k>l$. The demixing matrix obtained by UWEDGE is regarded as the initial value of the demixing matrix $\boldsymbol{W}^{[0]}$ in WEDGE.

Step 2: Iteration times: 1,2,…until final convergence.

Firstly, calculate $\hat{\boldsymbol{R}}_S[m] = \hat{\boldsymbol{W}}^{[i-1]}\hat{\boldsymbol{R}}_X[m](\hat{\boldsymbol{W}}^{[i-1]})^T$, m=0, 1, 2,…, M-1;

Secondly, calculate:

$$\hat{\boldsymbol{r}}_{kl} = [(\hat{\boldsymbol{R}}_s[0])_{kl}, (\hat{\boldsymbol{R}}_s[1])_{kl}, ..., (\hat{\boldsymbol{R}}_s[M-1])_{kl}]^T ,$$

where $k,l = 0,1,...,N, k>l$;

Thirdly, letbe $\hat{\boldsymbol{A}}^{[1]} = \boldsymbol{I}$. All non-diagonal elements in $\hat{\boldsymbol{A}}^{[1]}$ are replaced by (21):

$$\begin{bmatrix} \hat{\boldsymbol{A}}_{kl}^{[1]} \\ \hat{\boldsymbol{A}}_{lk}^{[1]} \end{bmatrix} = \begin{bmatrix} \hat{\boldsymbol{r}}_{ll}^T\boldsymbol{V}_{kl}\hat{\boldsymbol{r}}_{ll} & \hat{\boldsymbol{r}}_{kk}^T\boldsymbol{V}_{kl}\hat{\boldsymbol{r}}_{ll} \\ \hat{\boldsymbol{r}}_{kk}^T\boldsymbol{V}_{kl}\hat{\boldsymbol{r}}_{ll} & \hat{\boldsymbol{r}}_{kk}^T\boldsymbol{V}_{kl}\hat{\boldsymbol{r}}_{kk} \end{bmatrix}^{-1} \begin{bmatrix} \hat{\boldsymbol{r}}_{ll}^T\boldsymbol{V}_{kl}\hat{\boldsymbol{r}}_{kl} \\ \hat{\boldsymbol{r}}_{kk}^T\boldsymbol{V}_{kl}\hat{\boldsymbol{r}}_{kl} \end{bmatrix} \tag{21}$$

Fourthly, iteration process: $\hat{\boldsymbol{W}}^{[i]} = (\hat{\boldsymbol{A}}^{[1]})^{-1}\hat{\boldsymbol{W}}^{[i-1]}$;

Fifthly, normalize each row of $\hat{\boldsymbol{W}}^{[i]}$;

When i=i_{end}, the final demixing matrix is denoted as $\hat{\boldsymbol{W}} = \hat{\boldsymbol{W}}^{i_{end}}$.

D. Criteria for Evaluating the Effect of BSS

The similarity coefficient matrix can directly show the effect of BSS. The expression is [10]:

$$\varepsilon_{ij} = \varepsilon(y_i, s_j) = \frac{\left|\sum_{i=1}^{N} y_i(t)s_j(t)\right|}{\sqrt{\sum_{i=1}^{N} y_i^2(t)\sum_{j=1}^{N} s_j^2(t)}} \tag{22}$$

ε_{ij} describes the similarity between ith separated signal $y_i(t)$ and jth original signal $s_j(t)$. The corresponding value ε is close to 1 when separation effect is satisfying.

IV. Improving BSS Quality by Wavelet Denoising

The internal noise of the sensor should not be ignored in practice, and the effect of BSS algorithm is easy to be affected by channel noise. The mixing process containing channel noise is expressed as:

$$\begin{bmatrix} v_m(t) \\ v_a(t) \end{bmatrix} = \boldsymbol{A}\begin{bmatrix} S'(t) \\ J'(t) \end{bmatrix} + \begin{bmatrix} n_1(t) \\ n_2(t) \end{bmatrix} \tag{23}$$

where $n_1(t)$ and $n_2(t)$ are Gauss white noise in the channel. In order to reduce the influence of channel noise on the separation effect, wavelet de-noising is carried out on observed signals of the main and auxiliary antennas in this paper, and then WASOBI is used.

The wavelet de-noising of one dimensional signals usually includes three steps. First of all, wavelet decomposition layers *Num* is selected to decompose the signal by one dimensional wavelet decomposition. Then, the appropriate threshold value is selected and the high frequency wavelet coefficients from the first layer to the *Num*th layer are quantified. At last, the one-dimensional signal is reconstructed from the low-frequency wavelet coefficients of the *Num*th layer and the high-frequency wavelet coefficients from the first to the *Num*th layer after the threshold quantization [13].

The signal-to-noise ratio (SNR) is used to evaluate the de-noising effect as follows [13]:

$$SNR = 10\log\left[\frac{\sum_K x^2(n)}{\sum_K \left[x(n) - x'(n)\right]^2}\right] \tag{24}$$

where $x(n)$ represents the original noised signal. $x'(n)$ is the de-noised signal. K is the signal length.

V. Simulation and Analysis

To illustrate the effectiveness of the algorithm we proposed on separating smart noise jamming and target echo, some simulation experiments are carried out. In simulations, the enemy fighter plane carries the jammer, and the self-defense smart noise jamming is utilized to attack our radar. $\lambda=$ 0.1m, P_t =40kw, $g_m = 30dB$, $g_a = 10dB$. Radar main antenna is horizontal polarization, $\boldsymbol{h_m} = [1,0]^T$. Auxiliary antenna is vertical polarization, $\boldsymbol{h_a} = [0,1]^T$. Radar transmits LFM signal, pulse width is 50us, PRI is 500us. Bandwidth is $B = 5M$ and is processed as zero intermediate frequency. P_j =70w. The jammer antenna is circular polarization, $\boldsymbol{h_j} = \frac{1}{\sqrt{2}}[j,1]^T$. The narrowband noise bandwidth of jammer is 2M. The jamming duration is equal to the LFM signal pulse width, and $\tau_J = 50ns$. $R_j = 10km$, $\boldsymbol{S_p} = \frac{1}{2}\begin{bmatrix} 1 & j \\ j & -1 \end{bmatrix}$. Neglecting the change of target RCS, $\sigma = 10m^2$. The relative radial velocity of radar platform and target is 50m/s, showing a trend of approaching. The simulation is conducted on the signal in one PRI.

A. Noise-Free Case

The observed signals received by main and auxiliary antennas are shown in Fig. 2 respectively. Fig. 3 shows the result of pulse compression of radar received signals with and without jamming. From Fig. 3 (b), it can be seen that smart noise jamming inundates the real target echo, and a false target group may be formed at some distance, which has double interference characteristics of both suppression and deception.

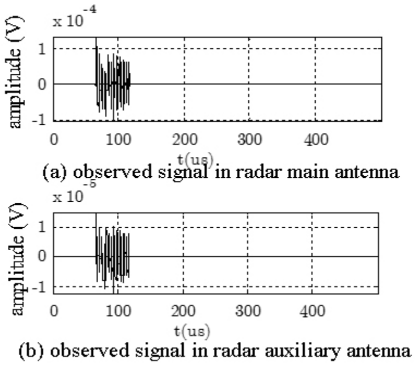

Figure 2. Receiving signals in main channel and auxiliary channel.

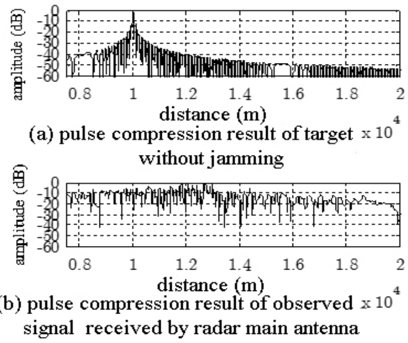

Figure 3. Pulse compression results of receiving signals (with jamming and without jamming).

The result of separating target echo and smart noise jamming by using WASOBI algorithm is shown in Fig. 4. Fig. 5 shows the results of pulse compression on two separated signals.

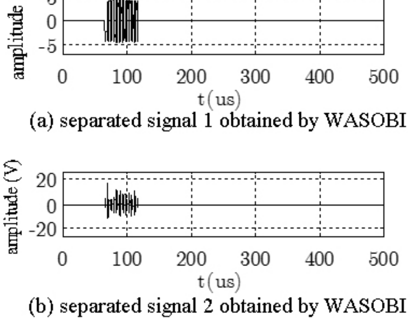

Figure 4. Separated signals by WASOBI.

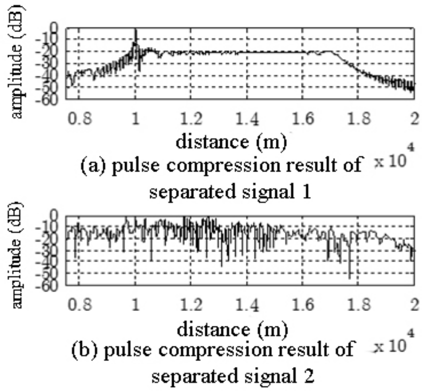

Figure 5. Pulse compression results of the separated signals.

The similarity coefficient matrix obtained by this separation is $\begin{bmatrix}0.9999 & 0.0917\\ 0.2066 & 0.9919\end{bmatrix}$. From the similarity coefficient matrix and Fig. 4, we can see that the separation of target echo and interference signal by WASOBI is successful. From the result of pulse compression in Fig. 5 (a), the distance information of the target has been obtained, and interference suppression ratio is about 12dB. In 100 independent experiments, the average value of the target echo similarity coefficient is 0.9932 and the jamming signal is 0.9846. We can conclude that the WASOBI algorithm can achieve a stable separation effect on target echo and smart noise jamming under noise-free condition.

B. Noise-Containing Case

The wavelet de-noising is used on the observed signals from the main and auxiliary antenna when channel noise is considered, and the heuristic threshold principle is selected. In this paper, orthogonal wavelet Daubechies6 is chosen to decompose the observed signal with 5 layers of wavelet.

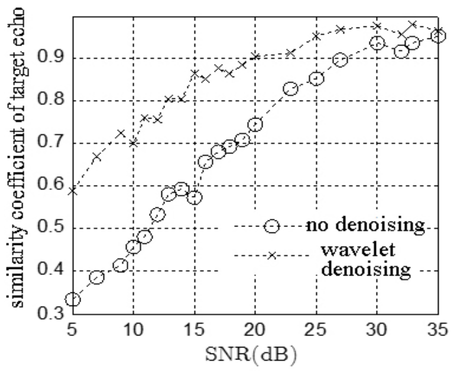

Figure 6. Similarity coefficient curve of target echo after separation.

Fig. 6 and Fig. 7 show the similarity coefficients of target echoes and jamming signals under different SNRs. The similarity coefficients in the graph are obtained from the average of 100 independent experimental results. It is known from the graph that noise in receiving channels has a great influence on BSS. With the increase of SNR, the similarity coefficient of the target echo increases gradually, which means the separation results of echo and jamming become better. The separation effects of the observed signals are improved by wavelet de-noising. When SNR>15dB, the similarity coefficient of target echoes can reach over 0.85. Smart noise jamming is easier to be extracted than the target echo, and its similarity coefficient is obviously superior to target echo. Therefore, WASOBI can also be used to extract this particular kind of interference signal. From Fig. 8, we can see that after de-noising, the interference suppression ratio of WASOBI algorithm is about 13dB under the condition of SNR=15dB.

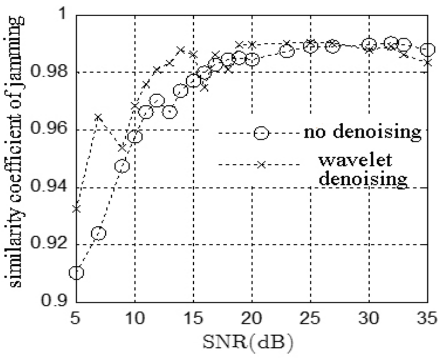

Figure 7. Similarity coefficient curve of jamming signal after separation.

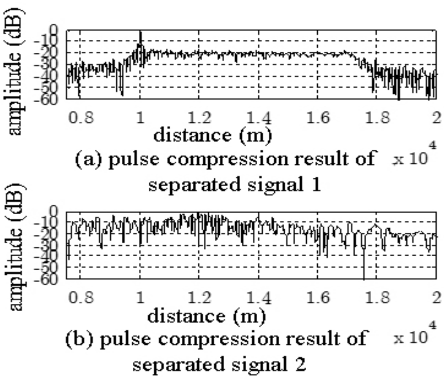

Figure 8. Pulse compression results of separated signals, when SNR=15dB.

VI. CONCLUSION

Aiming at the scene of self-defense jamming, this paper uses the polarization difference between the radar main antenna and the auxiliary antenna, and constructs the second mixing signal through the auxiliary antenna, which is orthogonal to radar main antenna. This method simplifies the single channel BSS problem. Firstly, the wavelet de-noising is carried out on the observed signals, and then the mixed signal is separated by WASOBI. The simulation results show that when SNR is greater than 15dB in receiving channel, the similarity coefficient of the target echo can reach more than 0.85, and the correct estimation of target distance can be obtained.

In this paper, a preliminary study on the separation of smart noise jamming and target echo is implemented. Further researches need to be carried on about whether other forms of smart noise jamming can be suppressed by BSS. In addition, whether other de-noising methods can help improve the performance of BSS is also worth exploring.

REFERENCES

[1] D. C. Schleher, *Electronic Warfare in the Information Age*, the United States: Artech House, 1999.

[2] M. Y. Feng, M. H. He, C. L. Yu, and B. Q. Wang, “Effects of adaptive sidelobe canceling against smart noise jamming,”. *Modern Defense Technology*, vol. 42, no. 3, pp. 5-8, Dec. 2014.

[3] J. Q. Ren, “Jamming suppression technology in LFM radars,” Ph.D. dissertation, University of Science and Technology of China, Anhui, China, 2017.

[4] S. C. Luo, and B. Tang, “An algorithm of deception jamming suppression based on blind signal separation,” *Journal of Electronics & Information Technology*, vol. 33, no. 12, pp. 2801-2806, Dec. 2011.

[5] H. W. Yin, G. L. Li, and C. H. Lu, “ Single-channel LFM fuze deception jamming suppression based on BSS,” *Telecommunication Engineering*, vol. 54, no. 11, pp. 1475-1481, Nov. 2014.

[6] W. Dong, X. B. Li, L. Shan, and Y. Wang, “An algorithm of radar mainlobe deception jamming suppression,” *Modern Defense Technology*, vol. 45, no. 2, pp. 209-216, April 2017.

[7] X. Li, C. Y. Wang, X. L. Fu, and H. Yuan, “Shift-frequency jamming suppression technique based on polarized channel expanding and blind source separation union,” *Journal of Beijing University of Aeronautics and Astronautics*, vol. 43, no. 4, pp. 731-737, July 2017.

[8] X. D. Han, W. X. Yu, T. Shu, and B. Tang, “Research on noise jamming to LFM signal radar,” *Computer Simulation*, vol. 31, no. 12, pp. 5-8, Dec. 2014.

[9] Y. Z. Li, G. Y. Wang, L. D. Wang, and X. S. Wang, “Study on polarization cancellation algorithm of self-defensive blanket jamming based on radar sidelobe-canceller antenna,” *Signal Processing*, vol. 24, no. 5, pp. 775-779, Oct. 2008.

[10] X. C. Yu, *The Theory and Application of Blind Source Separation*, Beijing: Science Press, 2011.

[11] P. Tichavsky, E. Doron, A. Yeredor, and J. Nielsen, “A computationally affordable implementation of an asymptotically optimal BSS algorithm for AR sources,” in *Proc. 14th European Signal Processing Conference*, Florence, Italy, 2006.

[12] P. Tichavsky and A. Yeredor, “Fast approximate joint diagonalization incorporating weight matrices,” *IEEE Transactions on Signal Processing*, vol. 57, no. 3, pp. 878-891, March 2009.

[13] K. Tao and J. J. Zhu, “A comparative study on validity assessment of wavelet de-noising,” *Journal of Geodesy and Geodynamics*, vol. 32, no. 2, pp. 128-133, April 2012.

Wen Yu received her M.S. degree in Information and Communication Engineering from Beihang University, China, in 2019.

Wei Chen received his Ph.D. degree from Beijing Institute of Technology, China, in 1997. Currently, he is an associate professor at School of Electronic Information Engineering in Beihang University. His research interests include Signal and Information Processing, Multi-sensor Information Fusion, Digital Image Processing, Intelligent Information Processing, etc.